SNOW WATER EQUIVALENT ESTIMATION USING DIFFERENTIAL SAR INTERFEROMETRY AND CO-POLAR PHASE DIFFERENCES FROM AIRBORNE SAR DATA

Kristina Belinska[a,b], Georg Fischer[a], Thomas Nagler[c], Irena Hajnsek[a,b]

[a] Microwaves and Radar Institute, German Aerospace Center (DLR), 82234 Wessling, Germany
[b] Institute of Environmental Engineering, ETH Zurich, 8092 Zurich, Switzerland
[c] ENVEO IT GmbH, 6020 Innsbruck, Austria

ABSTRACT

The Snow Water Equivalent (SWE) describes the amount of liquid water stored in a snow pack and is an important parameter for runoff predictions and flood forecasts. Differential Interferometric Synthetic Aperture Radar (DInSAR) can be used to estimate the SWE change between two temporally separated repeat pass SAR acquisitions utilizing the interferometric phase. However, only a limited range of SWE changes can be retrieved unambiguously due to phase wraps of the interferometric phase. In this study, the aim is to include information on snow depth obtained from the Co-polar Phase Difference (CPD) between the polarimetric channels to detect phase wraps and improve the SWE retrieval results. The investigations are performed using airborne SAR acquisitions over the Alps.

Index Terms— Synthetic Aperture Radar, SWE, Interferometric SAR, Polarimetric SAR

1. INTRODUCTION

The snow pack is an important variable for climate and hydrological models, as estimations of the amount of water contained in the snow are essential for runoff predictions [1] and flood forecasts [2]. A significant parameter for that is the Snow Water Equivalent (SWE), which describes the amount of liquid water stored in a snow pack.

A method proposed in [3] and later in [4] demonstrates the potential of Differential Interferometric Synthetic Aperture Radar (DInSAR) to measure the SWE change between two repeat-pass SAR acquisitions. The approach is based on the fact that microwaves are refracted in the snow pack, which induces a phase delay and has an effect on the interferometric phase. It can be shown physically, that the interferometric phase can be directly linked to the SWE change.

It has to be taken into consideration that this method has limitations because of the 2π ambiguity of the interferometric phase. This results in phase wraps when the SWE change exceeds a certain threshold. This threshold depends on the wavelength and is higher for longer wavelengths.

Moreover, the Co-polar Phase Difference (CPD) between the VV and HH polarimetric channels can be correlated to the depth of freshly accumulating snow [5]. The CPD can be modelled in dependence of snow anisotropy, density and depth [6] and thus can be used to invert the fresh snow depth. This can be included in the DInSAR SWE retrieval model to estimate the phase wraps and improve its performance.

The aim of this study is to include polarimetric variables in the DInSAR SWE retrieval algorithm to detect phase wraps. In doing so, the influence of different frequencies, C- and L-band is also assessed. The study is performed using airborne SAR data over the Austrian Alps.

2. METHODS

2.1. DInSAR Phase for SWE Estimation

In [3] and [4] a model is described, which uses differential interferometry to estimate the SWE change between two SAR images, which are separated by a temporal baseline. Due to the fact that snow has a different refractive index than air, radar waves are refracted, as shown in Fig. 1.

The path delay of the radar wave is proportional to the snow depth change ΔZ_S between the two acquisitions and can be translated into the phase difference $\Delta\Phi_S$ using the geometry in Fig. 1:

$$\Delta\Phi_s = -2\, k_i \Delta Z_s \left(\cos\Theta - \sqrt{\epsilon - \sin\Theta^2}\right) \qquad (1)$$

Here, $k_i = 2\pi/\lambda$ is the wavenumber of the wavelength λ, Θ describes the incidence angle of the radar wave and ϵ is the permittivity of the snow, which depends on the density.

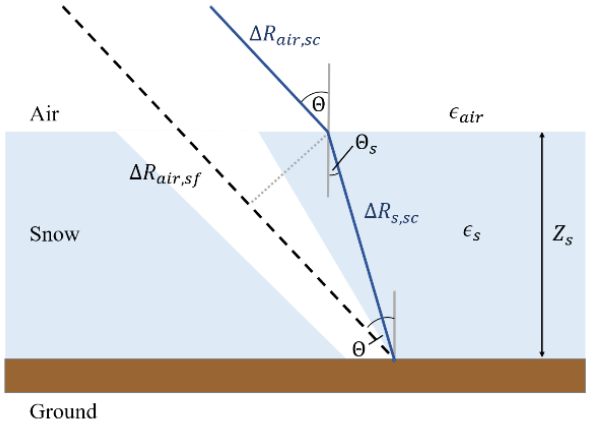

Figure 1 Path of the radar wave for snow (blue line) compared to snow free conditions (dotted line).

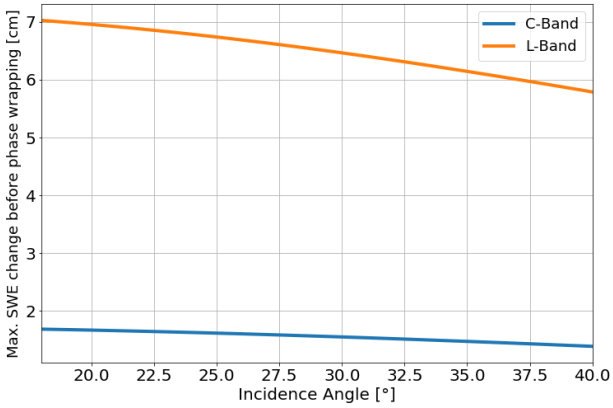

Figure 2 SWE change for a phase difference $\Delta\Phi_s = \pi$ in dependence of the incidence angle for C- and L-band. The equivalent thresholds apply for negative changes.

The authors in [4] showed numerically that the density and incidence angle-dependent part of the equation can be replaced and obtained the following relation between the phase and SWE change ΔSWE:

$$\Delta\Phi_s = 2\, k_i \frac{\alpha}{2} \left(1.59 + \Theta^{\frac{5}{2}}\right) \Delta SWE \qquad (2)$$

The parameter α lies close to 1 and can be adapted to reduce the Root Mean Square Error (RMSE) between the approximation and the exact solution [4].
However, in region with slopes due to topography, in-situ measurements are not measured perpendicular to the surface. Therefore, when comparing the retrieved SWE values with the ground measurements, the slope has to be considered and the retrieved SWE values have to be scaled accordingly.
The interferometric phase $\Delta\Phi_S$ lies in the interval between -π and π. Therefore, it is only possible to retrieve a limited range of ΔSWE unambiguously. When ΔSWE exceeds this interval, phase wraps occur which need to be determined for an accurate SWE retrieval. The upper boundary for the SWE retrieval is displayed in Fig. 2 for C- and L-band in dependence of the incidence angle. It can be seen, that the range for the ΔSWE retrieval is proportional to the wavelength.

2.2. CPD for Snow Depth Estimation

The Co-polar Phase Difference (CPD) Φ_{CPD} between the phase Φ_{VV} of the VV and the phase Φ_{HH} of the HH polarized channel can be defined as:

$$\Phi_{CPD} = \Phi_{VV} - \Phi_{HH}. \qquad (3)$$

In an anisotropic snow structure, the signal delay of the radar wave in the snow is polarization dependent. Freshly accumulating snow forms horizontal structures due to its own weight, leading to a decreased propagation velocity of horizontally polarized radar waves. In contrast, older snow forms vertical structures, because of recrystallization under temperature gradients, which has the effect of a slower propagation velocity of vertically polarized radar waves. Therefore, it is possible to relate positive CPDs to the fresh snow height [5].
The snow pack can be modelled as ellipsoidal ice inclusions in air. Using an empirical extension of the Maxwell-Garnett mixing formulas, the depolarization factors along the three main axes of the ice inclusions are computed for different assumptions of the anisotropy. The refractive indices of the horizontal polarized channel n_H and of the vertical polarized channel n_V can be calculated using the depolarization factors. The obtained expression for the CPD is then the following [6]:

$$\Phi_{CPD} = (-1)\frac{4\pi}{\lambda}\Sigma\Delta Z_s \left(\sqrt{n_V^2 - \sin^2(\Theta)} - \sqrt{n_H^2 - \sin^2(\Theta)}\right) \qquad (4)$$

For freshly accumulating snow the CPD is positive and becomes negative when the snow forms vertical structures. Therefore, the thickness of the fresh snow layer can be estimated. The relation between the CPD and the fresh snow depth will be analysed with the purpose to estimate if phase wrapping in the DInSAR phase has occurred.

3. TEST SITE AND F-SAR DATA

In the frame of the SARSimHT-NG study by ESA [7] airborne SAR data was acquired in March 2021 by DLR's airborne radar system F-SAR, accompanied by ground

measurements of snow properties [8]. The test site is located in the Austrian Alps in the Wörgetal. The F-SAR measurements were performed in C- and L-band and are quad-pol. The time series contains 8 acquisitions, acquired between the 02.03.2021 and 19.03.2021.

4. PRELIMINARY RESULTS

The interferometric coherences are calculated for each pair of two consecutive acquisitions of the acquired time series. In Fig. 3, the coherence amplitudes for the VV channel between the 02.03.2021 and 06.03.2021 acquisitions are shown. It can be seen, that coherence values are larger for L-band than for C-band.

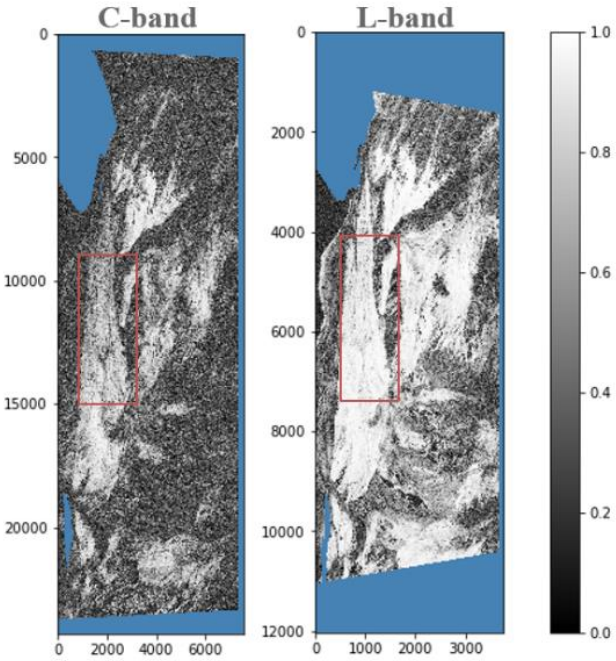

Figure 3 Coherence amplitude between the 02.03.2021 and 06.03.2021 acquisitions in radar coordinates for C-band (left) and L-band (right). The red rectangle shows the test site.

For both frequencies, the radar wave penetrates through the whole snow pack and therefore Eq. 2 can be used to calculate SWE change from the DInSAR phase after calibration using the phase of the corner reflectors. Due to the fact that ground-based measurements of snow depth and density were performed on the 02.03.2021 and 06.03.2021 and a snow fall event occurred on the 05.03.2021, the interferograms between the 02.03.2021 and 06.03.2021 were analyzed more in detail.

In Fig.4 the SWE change is shown for the test site. The black points correspond to in-situ measurements. In general, regions with low coherences are corresponding to noisy SWE estimation results. Moreover, the measurements in mountainous regions are also affected by layover and shadowing effects.

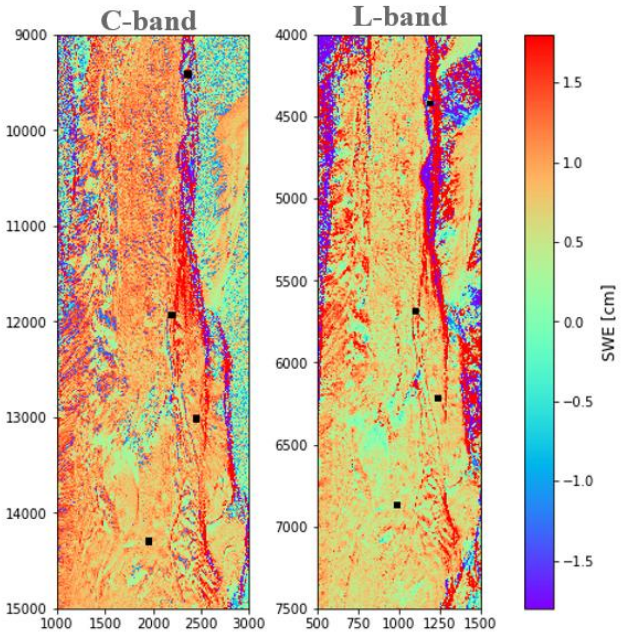

Figure 4 SWE change between the 02.03.2021 and 06.03.2021 acquisitions in radar coordinates for C-band (left) and L-band (right). Zoom-in on the test site. Black points correspond to in-situ measurements reported in Tab. 1 and 2.

The resulting SWE changes are compared to the ground measurements in Table 1 for C-band and Table 2 for L-band. In general, the coherences in VV and HH are higher in L-band. The DInSAR SWE estimates at T41, T42 and T52 are very close to the in-situ measurements. Only T51 strongly deviates from the ground measurements, but is also the point with the lowest coherence.

Table 1 DInSAR retrieved SWE change for the VV and HH channels between the 02.03.2021 and 06.03.2021 for C-band.

Point	Coh VV	Coh HH	SWE VV [cm]	SWE HH [cm]	In-Situ [cm]
T41	0.73	0.74	1.01	1.02	1.19
T42	0.68	0.73	0.99	0.95	1.05
T51	0.23	0.26	1.83	0.17	0.94
T52	0.58	0.56	1.08	1.19	1.19

Table 2 DInSAR retrieved SWE change for the VV and HH channels between the 02.03.2021 and 06.03.2021 for L-band.

Point	Coh VV	Coh HH	SWE VV [cm]	SWE HH [cm]	In-Situ [cm]
T41	0.93	0.94	0.93	1.09	1.19
T42	0.86	0.90	1.21	0.81	1.05
T51	0.52	0.55	3.52	4.96	0.94
T52	0.95	0.95	0.90	1.07	1.19

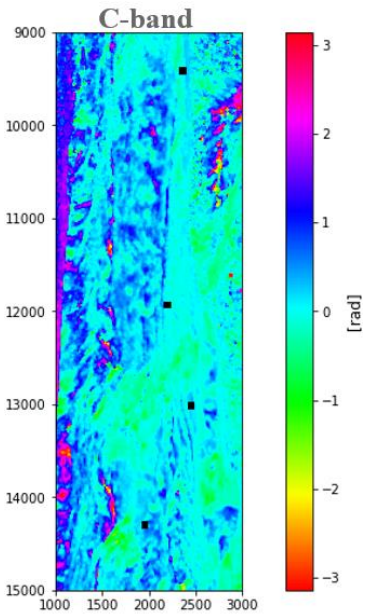

Figure 5 CPD in [rad] for the 06.03.2021 in radar coordinates for C-band. Zoom-in on the test site.

Additionally, the CPD is shown for 06.03.2021 in Fig. 4. The positive CPD values indicate that there is a layer of fresh snow with a horizontal structure, while regions with a CPD of zero indicate that no fresh snow has accumulated. By applying Eq. (4) at the in-situ points it is checked, whether a phase wrap is predicted using the CPD. It is tested for C-band assuming a density of 0.1 and snow anisotropy of 0.2. The results for all 4 points indicate that no phase wrapping occurred which is in accordance with the in-situ measurements.

5. OUTLOOK

The high coherence amplitudes between two F-SAR acquisitions demonstrate the potential for the SWE retrieval using the interferometric phase. Here, when comparing SWE retrieval results to the in-situ measurements for C- and L-band, a good agreement for the points with a high coherence can be achieved. Additionally, the CPD values over the test site are used to retrieve the fresh snow depth in order to detect whether DInSAR-phase wraps have occurred. This has been first tested for the C-band measurements, but will be also validated with more ground measurements for both frequencies.

6. ACKNOWLEDGEMENT

The authors would like to thank the DLR F-SAR team for the acquisition of the airborne SAR data and the ground team from ENVEO for collecting in-situ measurements.

7. REFERENCES

[1] T. P. Barnett, J. C. Adam, and D. P. Lettenmaier, “Potential impacts of a warming climate on water availability in snow-dominated regions,” *Nature*, vol. 438, no. 7066, pp. 303–309, Nov. 2005, doi: 10.1038/nature04141.

[2] S. S. Carroll, G. N. Day, N. Cressie, and T. R. Carroll, “Spatial modelling of snow water equivalent using airborne and ground-based snow data,” *Environmetrics*, vol. 6, no. 2, pp. 127–139, Mar. 1995, doi: 10.1002/env.3170060204.

[3] T. Guneriussen, K. A. Hogda, H. Johnsen, and I. Lauknes, “InSAR for estimation of changes in snow water equivalent of dry snow,” *IEEE Transactions on Geoscience and Remote Sensing*, vol. 39, no. 10, pp. 2101–2108, Oct. 2001, doi: 10.1109/36.957273.

[4] S. Leinss, A. Wiesmann, J. Lemmetyinen, and I. Hajnsek, “Snow Water Equivalent of Dry Snow Measured by Differential Interferometry,” *IEEE Journal of Selected Topics in Applied Earth Observations and Remote Sensing*, vol. 8, no. 8, pp. 3773–3790, Aug. 2015, doi: 10.1109/JSTARS.2015.2432031.

[5] S. Leinss, G. Parrella, and I. Hajnsek, “Snow Height Determination by Polarimetric Phase Differences in X-Band SAR Data,” *IEEE J. Sel. Top. Appl. Earth Observations Remote Sensing*, vol. 7, no. 9, pp. 3794–3810, Sep. 2014, doi: 10.1109/JSTARS.2014.2323199.

[6] S. Leinss, H. Löwe, M. Proksch, J. Lemmetyinen, A. Wiesmann, and I. Hajnsek, “Anisotropy of seasonal snow measured by polarimetric phase differences in radar time series,” *The Cryosphere*, vol. 10, no. 4, pp. 1771–1797, Aug. 2016, doi: 10.5194/tc-10-1771-2016.

[7] V. Grachea, R. Horn, T. Nagler, and J. Fischer, “SARSimHT-NG – Simulation of Hydroterra SAR System Performance in the Mediterranean and the Alps Based on Experimental Airborne SAR Data,” DLR, Enveo, ESA Airborne Campaign 2021-2022.

[8] T. Nagler *et al.*, “Field Campaigns on InSAR retrieval of snow mass in preparation of Copernicus ROSE-L,” submitted to Living Planet Symposium, 2022.